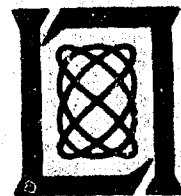| Technical Note	1980-45
	S. D. Weiner
A Model of Interceptor Engagements Including Warhead and Fuze Interactions	
	18 September 1980
Prepared for the Department of the Army under Electronic Systems Division Contract F19628-80-C-0002 by	

Lincoln Laboratory

MASSACHUSETTS INSTITUTE OF TECHNOLOGY

LEXINGTON, MASSACHUSETTS

80 12 24 046

The views and conclusions contained in this document are those of the contractor and should not be interpreted as necessarily representing the official policies, either expressed or implied, of the United States Government.

This technical report has been reviewed and is approved for publication.

FOR THE COMMANDER

Joseph C. Syiek
Project Officer
Lincoln Laboratory Project Office

MASSACHUSETTS INSTITUTE OF TECHNOLOGY

LINCOLN LABORATORY

A MODEL OF INTERCEPTOR ENGAGEMENTS
INCLUDING WARHEAD AND FUZE INTERACTIONS

S. D. WEINER

Group 32

TECHNICAL NOTE 1980-45

18 SEPTEMBER 1980

LEXINGTON   MASSACHUSETTS

ABSTRACT

This note represents an extension of previous work on radar homing interceptors to include effects of multiple sensor interactions and the use of aimed warheads to compensate for large guidance miss-distances. Using simple graphical techniques, we treat combinations of data from handover, homing and fuzing sensors. We also consider various types of warheads including isotropic, aimed in one angle, fully aimable and fully aimable and chokable. Sensors are characterized by their accuracy and acquisition range; interceptors by their maneuver capability and response time and warheads by their reach, coverage and response time. We consider some sample intercept engagements and discuss their component requirements.

Accession For

NTIS GRA&I
DTIC TAB
Unannounced
Justification

By
Distribution/
Availability Codes
Avail and/or
Dist | Special

CONTENTS

I. INTRODUCTION

This note is an extension of the work presented in Ref. [1]. In that report, we discussed a graphical model for evaluating miss-distance for homing interceptors to perform non-nuclear kill (NNK) of ballistic re-entry vehicles. By comparing the homing sensor prediction accuracy with the interceptor divert capability as a function of time (or range) to go, it is possible to estimate the handover accuracy requirements and the resulting miss distance. Here we will indicate how the model can be modified to include data from multiple sensors and to account for the ability of an aimed warhead to operate with relatively large guidance miss-distances. We will briefly describe the model of Ref. [1] but the interested reader is encouraged is consult that report for details of the technique.

In Section II we review the sensor model of Ref [1] indicating how data from different sensors can be combined to determine the resulting prediction accuracy. Section III contains a review of the interceptor model of Ref. [1]. In Section IV, we discuss the functions of the NNK warhead in compensating for large guidance miss-distances which become known too late for interceptor maneuvers to correct. We consider various types of isotropic and aimed warheads and characterize them in terms of reach, coverage and response time. All these component models are combined in Section V to make an overall model for evaluating

system performance. We consider a number of sample engagements
to indicate which subsystem parameters influence which aspect of
the engagement. These include handover, homing (interceptor
guidance) and fuzing (warhead aiming and firing). Finally we
summarize the conclusions in Section VI.

As mentioned in Ref. [1], it is important to remember
that this model is highly simplified. Its primary purpose is to
illustrate the interaction among various subsystem parameters
rather than to give precise numerical results.

II. SENSOR MODEL

In Ref. [1], we calculated the prediction error for a homing sensor which tracks a target from its acquisition range, R_A, to a given range, R, and predicts ahead to intercept (at range = 0). If the closing velocity is V_c and the seeker operates at a constant prf with a position measurement accuracy, σ_R, which is a function of range, then the variance of the estimate of the intercept point is

$$
\mathrm{Var}(a_0) = \frac{V_c}{prf} \frac{\displaystyle\int \frac{R^2}{\sigma_R^2}\,dR}{\displaystyle\int \frac{dR}{\sigma_R^2} \int \frac{R^2}{\sigma_R^2}\,dR - \left(\int \frac{R}{\sigma_R^2}\,dR\right)^2} \tag{1}
$$

where all integrals go from R_A to R. The prediction error is the square root of $\mathrm{Var}(a_0)$. Eq. (1) results from a linearized error analysis about the true trajectory. For this to be valid, we must have a good model of the target and interceptor dynamic response, particularly their acceleration characteristics. (Ref. [2] indicates how acceleration errors can be accommodated.)

In Ref. [1], we considered cross-range (angular) error to be the dominant contributor to σ_R and to be comprised of three components; glint, instrumentation and thermal errors. In Ref. [3],

3

it is shown that range errors contribute to $\text{Var}(a_0)$ but do not significantly affect the distance of closest approach. Thus, angle-only tracking using proportional navigation can insure that the interceptor passes close to the target but a fuze sensor which measures range is required to determine the time of closest approach with sufficient accuracy to make efficient use of a warhead.

In this report, we will concentrate on instrumentation error which is a constant angular error resulting in a position error which varies linearly with R.

$$\sigma_R = \sigma_\theta R \tag{2}$$

substituting (2) into (1) gives

$$\text{Var}(a_0) = \frac{V_c \sigma_\theta^2 R}{\text{prf}} \frac{y-1}{y+(1/y)-2-(\ln y)^2} \tag{3}$$

where $y \equiv R_A/R$. Again, prediction error is the square root of $\text{Var}(a_0)$. Results for other types of errors are given in Ref. [1]. Figure 1 shows how the prediction error varies with R and R_A for a sample set of parameters. Note that R_A strongly influences the accuracy at large R but much less so at small R.

In the rest of this section we will give a simple method for determining the prediction error when the target is tracked

4

by more than one sensor. For this purpose it is helpful to use the nomogram of Ref. [1] which is reprinted as Appendix A. We first consider the case of handover from a ground based radar.

Consider the seeker in Fig. 1, with R_A = 3km. Assume that a ground radar hands over a predicted intercept point which is accurate to 25 m. The results for this case are illustrated in Fig. 2. For R>3 km, only the handover data is available and the prediction error is 25 m. At R=3 km, the seeker starts making measurements with σ_θ=10 mr and can thus reduce the prediction error. In Fig. 2 it is seen that data from the seeker alone would not provide better prediction than 25 m until R decreased to 2 km. However by combining the seeker and handover data, better accuracy can be achieved. The dashed curve corresponding to R_A=5 km goes through the point at 3 km range and 25 m prediction accuracy. If we follow this curve for R<3 km, we have a very close approximation to the actual situation. From the viewpoint of what happens after R=3 km, the two cases listed below are virtually indistinguishable:

a)   seeker acquires at R=5 km, tracks with σ_θ=10 mr, achieves a prediction error of 25 m at R=3 km, continues to track with σ_θ=10 mr.

b)   Target is handed over with error of 25 m at R=3 km, seeker continues to track with σ_θ=10 mr.

In this case the heavy line in Fig. 2 corresponds to the prediction accuracy achieved using both handover and seeker data.

5
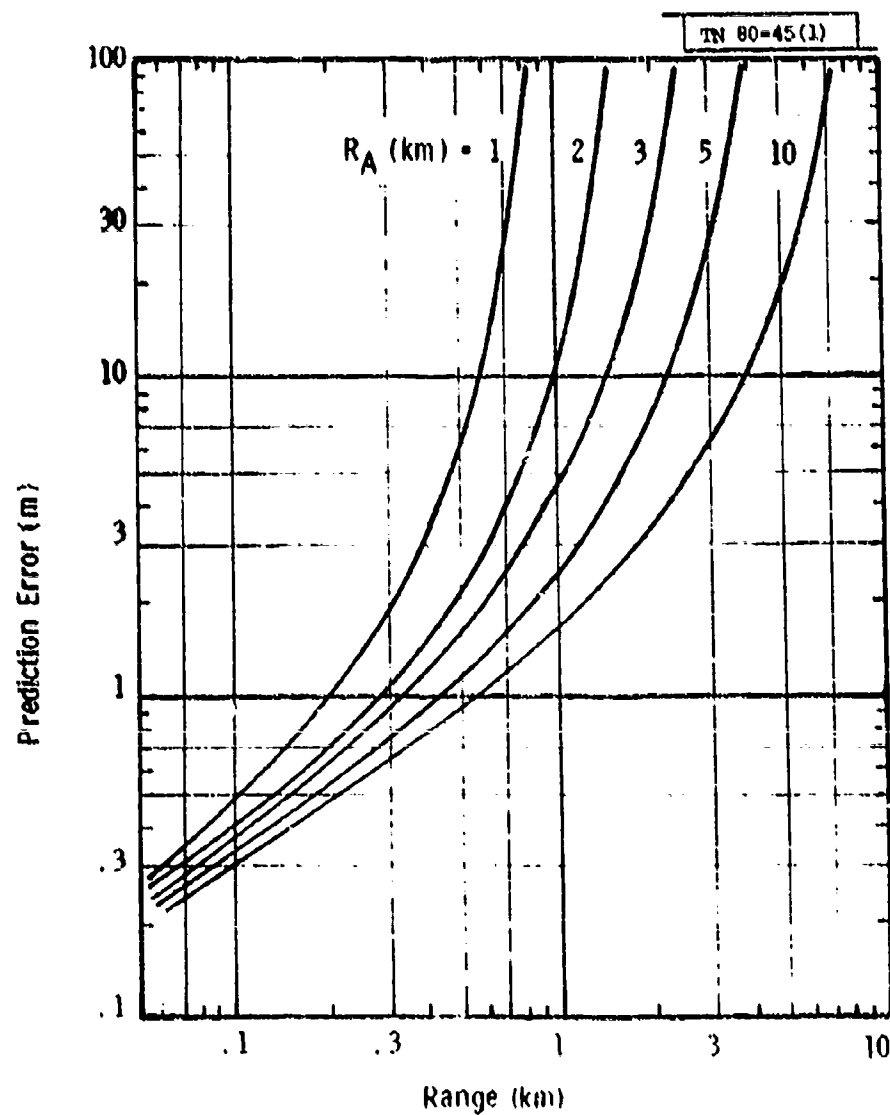
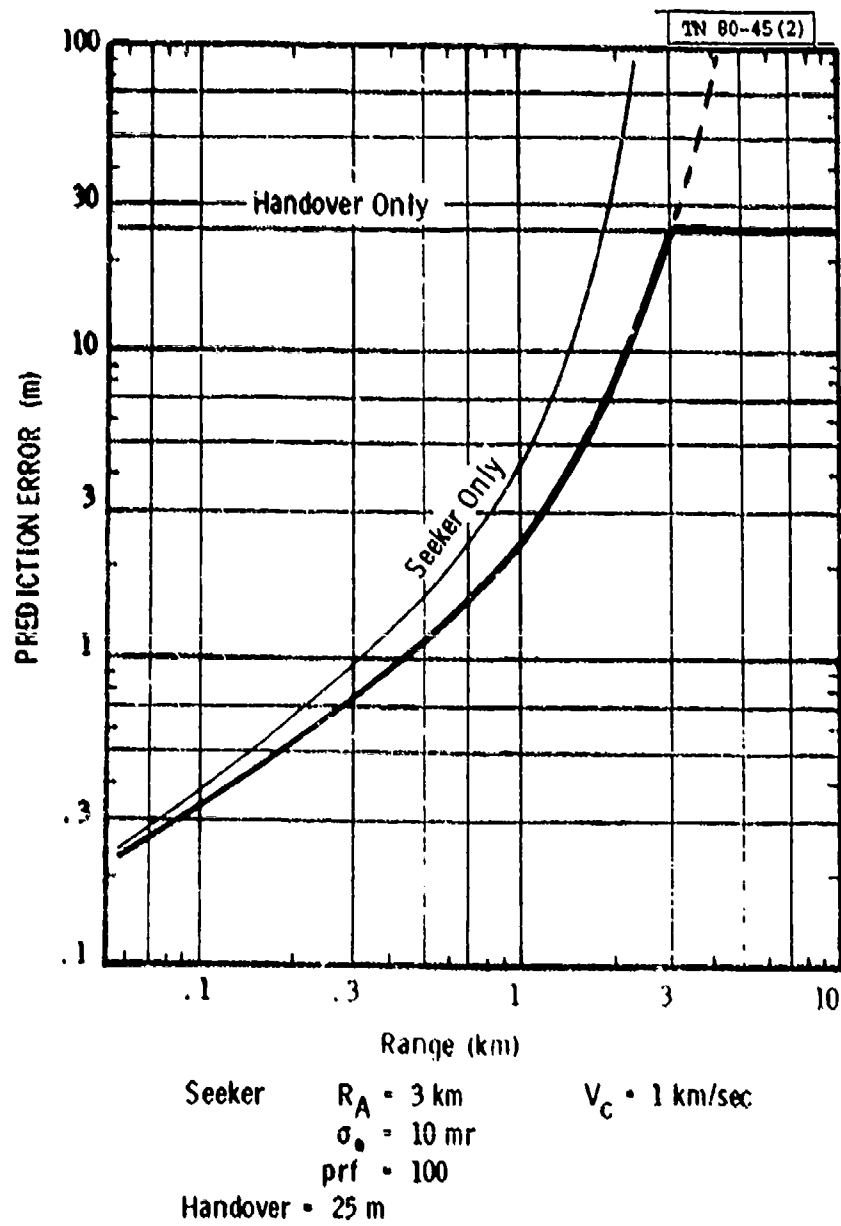Fig.1. Prediction error.

Fig. 2.   Combined handover-seeker data.

We can use exactly the same technique for combining data from a longer-range, less-accurate seeker and a shorter-range, more-accurate fuze. Figure 3 illustrates the case considered. The seeker tracks from R=5 km to R=1 km with σ_θ=10 mr achieving a prediction error of about 2.5 m. At this point the fuze acquires and tracks with an accuracy of 2 mr. The resulting performance for R<1 km is as if the fuze acquired at about 1.8 km range since this hypothetical sensor has a prediction error of 2.5 m at 1 km range. Again the heavy line corresponds to the prediction accuracy using both seeker and fuze data.

This technique can be applied for any number of sensor handovers and also for glint and thermal errors.
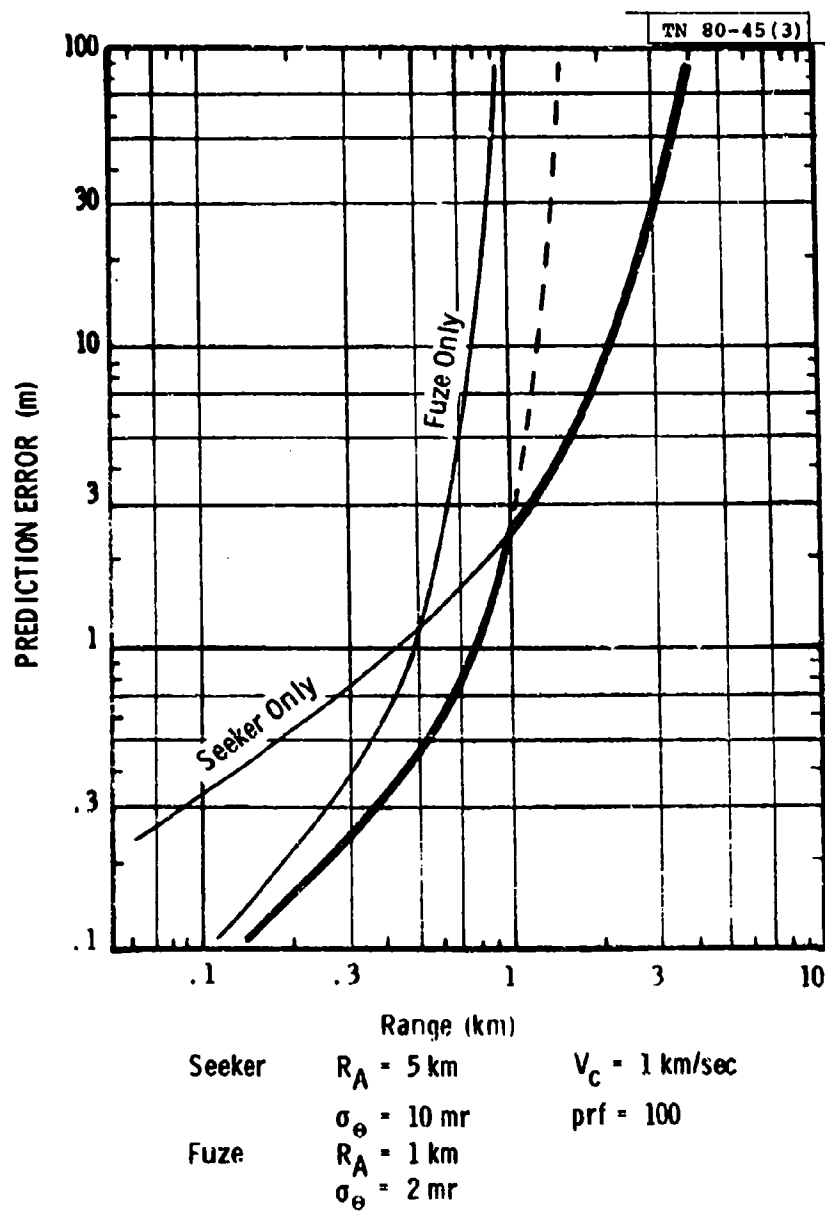
PREDICTION ERROR (m)

Fuze Only

Seeker Only

Range (km)

Seeker	R_A = 5 km	V_c = 1 km/sec
	σ_Θ = 10 mr	prf = 100
Fuze	R_A = 1 km	
	σ_Θ = 2 mr	

Fig. 3. Combined seeker-fuze data.

III. INTERCEPTOR MODEL

The interceptor model used is identical with that of Ref. [1]. The interceptor has a response time, τ, and a maximum maneuver acceleration limit, a. When a maneuver is commanded, we model the missile response as being zero for a time τ followed by constant acceleration, a, for the time required or the time remaining, whichever is less. The maximum divert which can be achieved is given by

$$\text{Divert} = \frac{a}{2} \left(\frac{R}{V_c} - \tau \right)^2 \tag{4}$$

This is graphed in Fig. 4.

Divert Capability (m)

100

.30

10

3

1

τ (sec) = .1 .2 .3 .5

.3

.1

.1 .3 1 3 10

Range (km)
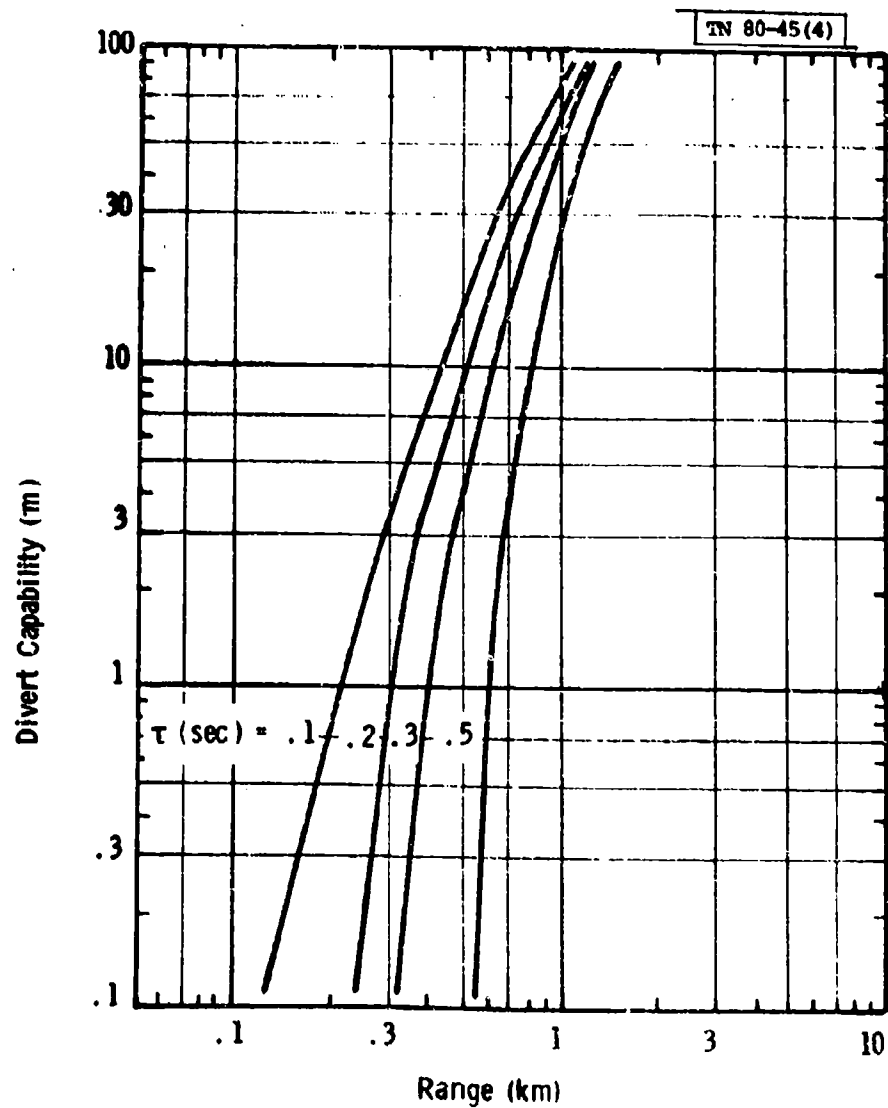
a = 20 g
V_c = 1 km/sec

Fig. 4. Interceptor divert.

11

IV. WARHEAD MODEL

The final component we will model is the fragmentation
warhead. To appreciate the factors which enter into warhead
design, it is necessary to understand what happens in a homing
engagement. Figure 5 illustrates the various components of the
miss-distance near the time of warhead fuzing. Shown is the
"miss-plane" perpendicular to the relative interceptor-target
velocity in interceptor-fixed coordinates. The interceptor is
guided to a point offset by some distance (which may be zero) from
the point of closest approach. The lightly shaded circle represents
the potential guidance error in achieving the desired geometry.
This is the miss-distance discussed in Ref. [1] and results from a
combination of homing sensor errors and finite interceptor res-
ponse time; the interceptor has insufficient maneuver capability
to cover the predicted target uncertainty volume. However as the
engagement progresses, the sensors (seeker or fuze or both) continue
to make measurements. As the relative range decreases, both the
sensor error and the prediction time decrease, significantly
decreasing the predicted uncertainty volume. This can be seen in
Figs. 2 and 3. While the interceptor itself cannot take advantage
of this reduced uncertainty, the warhead may be able to if it is
sufficiently responsive. At the time of warhead fuzing, the un-
certainty volume may have shrunk to the size of the darkly shaded
circle in Fig. 5. In this case, the warhead need only cover this

12

Target

Target Velocity Relative
To Interceptor

Miss Plane
Perpendicular To
Relative Velocity

Miss Bias

Unknown Error

Known Error

Envelope Of Potential
Engagement Error

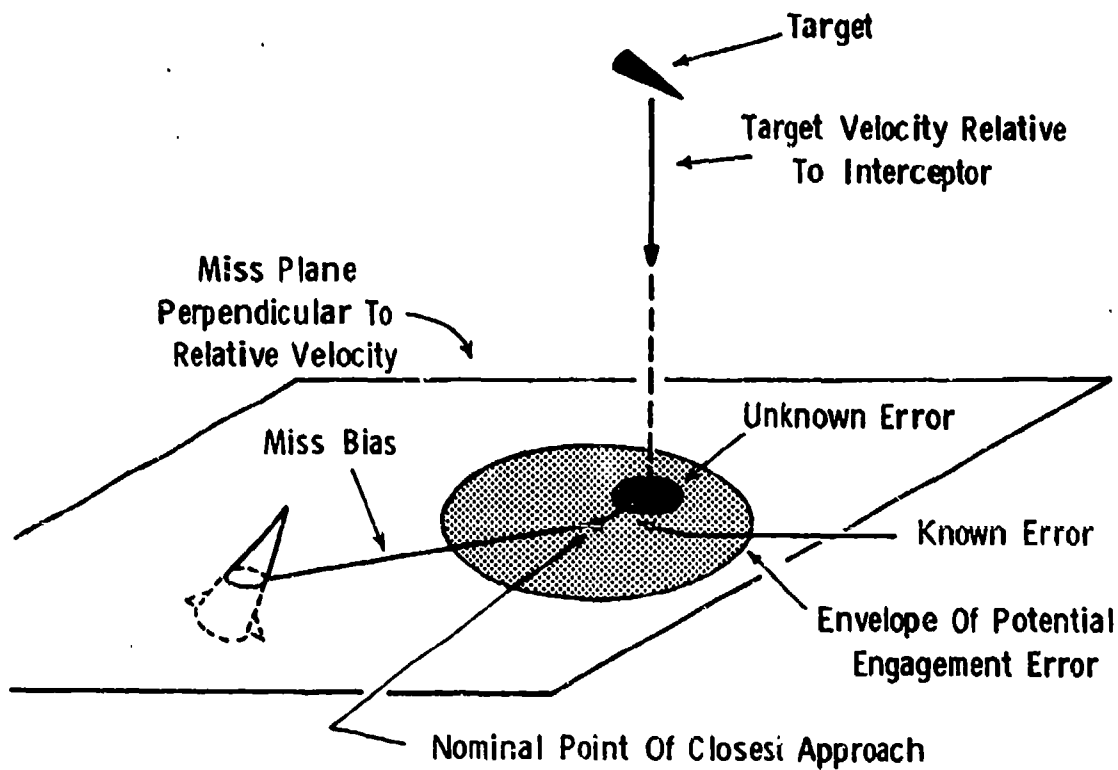Nominal Point Of Closest Approach

Fig. 5. Types of miss-distance.

dark circle with fragments rather than the entire lightly shaded circle. The dark circle represents the fuze error and the target location within it remains unknown at fuzing time. The light circle represents the guidance error and the target location within this circle becomes known (to within the fuze error) at fuzing time. The warhead must be capable of covering the dark circle for any location of it within the light circle. Later we will relate these volumes to the concepts of warhead coverage and reach.

We will consider four classes of fragment warheads; isotropic, one-axis aimable, two-axis aimable, and two-axis aimable and chokable. Most practical warheads represent one or a combination of these classes (see Ref. [4]). An isotropic warhead puts out a spherical cloud of fragments centered on the interceptor. The aimed warheads put out a spray of fragments confined to a beam of fixed angular width Φ which can be directed anywhere in azimuth (for a one-axis warhead) or in both azimuth and elevation (for a two-axis warhead). For a chokable warhead, the beam spray angle can also be controlled.

For all warheads, the kill probability is a product of two factors. (See Ref. [5].) The first is the probability that the fragment pattern is large enough to envelop the uncertainty in location of the target (or the vulnerable area of the target). The second factor is the probability that the fragment pattern is dense enough to provide a sufficient number of hits on the target.

14

These factors are plotted as a function of the distance from the interceptor to the target for several warheads in Fig. 6. It is seen that narrowing the fragment beam increases the nomimal stand-off required and increases the spread of standoff distances which can be tolerated.

The spread in standoff distance permitted can be related to the acceptable guidance miss-distance for the various warhead types. This is illustrated in Fig. 7 for the one-axis and two-axis aimed warheads. (We show cases confined to the plane of the paper since both warheads can be aimed in azimuth to compensate for any out-of-plane error.) Since the kill must occur at one particular point for the one-axis aimed warhead, the guidance error which can be accommodated is equal to the spread in standoff distances which is permitted. The two-axis aimed warhead however can select a kill point anywhere within its maximum standoff range and thus can tolerate a larger guidance error which is equal to this maximum standoff distance. Since the maximum standoff distance increases with decreasing beam-spray angle, a chokable warhead can operate out to the standoff corresponding to its minimum spray angle. From Fig. 7, we see that the payoff for chokability may be greater for a 1-axis warhead than for a 2-axis warhead.

Thus far we have talked about the maximum guidance error the various warheads can accommodate. This can be thought of as the "reach" of the warhead. If this were the only performance measure, the the narrowest beamwidth two-axis aimable warhead
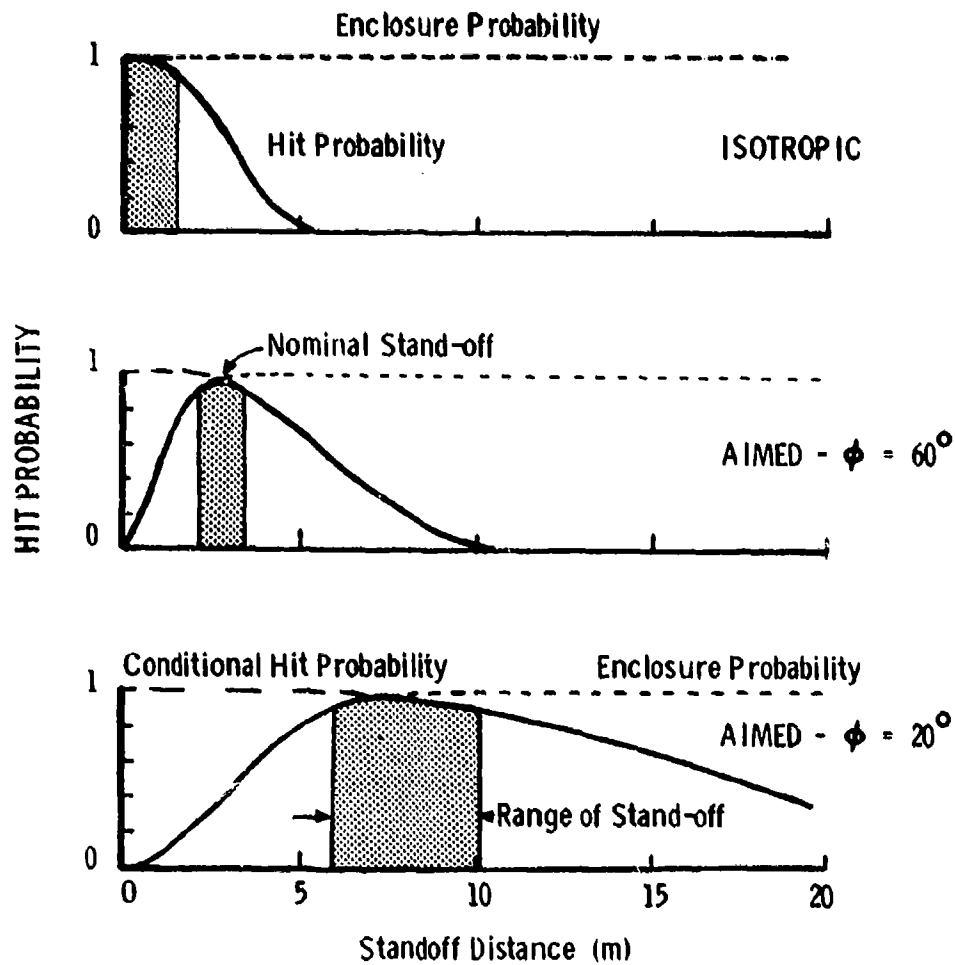
15

Fig. 6. Standoff requirements for various warheads.

16

Potential Targets

1 - AXIS AIMED W/H

Pattern
too small

Interceptor

Pattern
just right

Pattern
too sparse

2 - AXIS AIMED W/H

Pattern
just right

Pattern
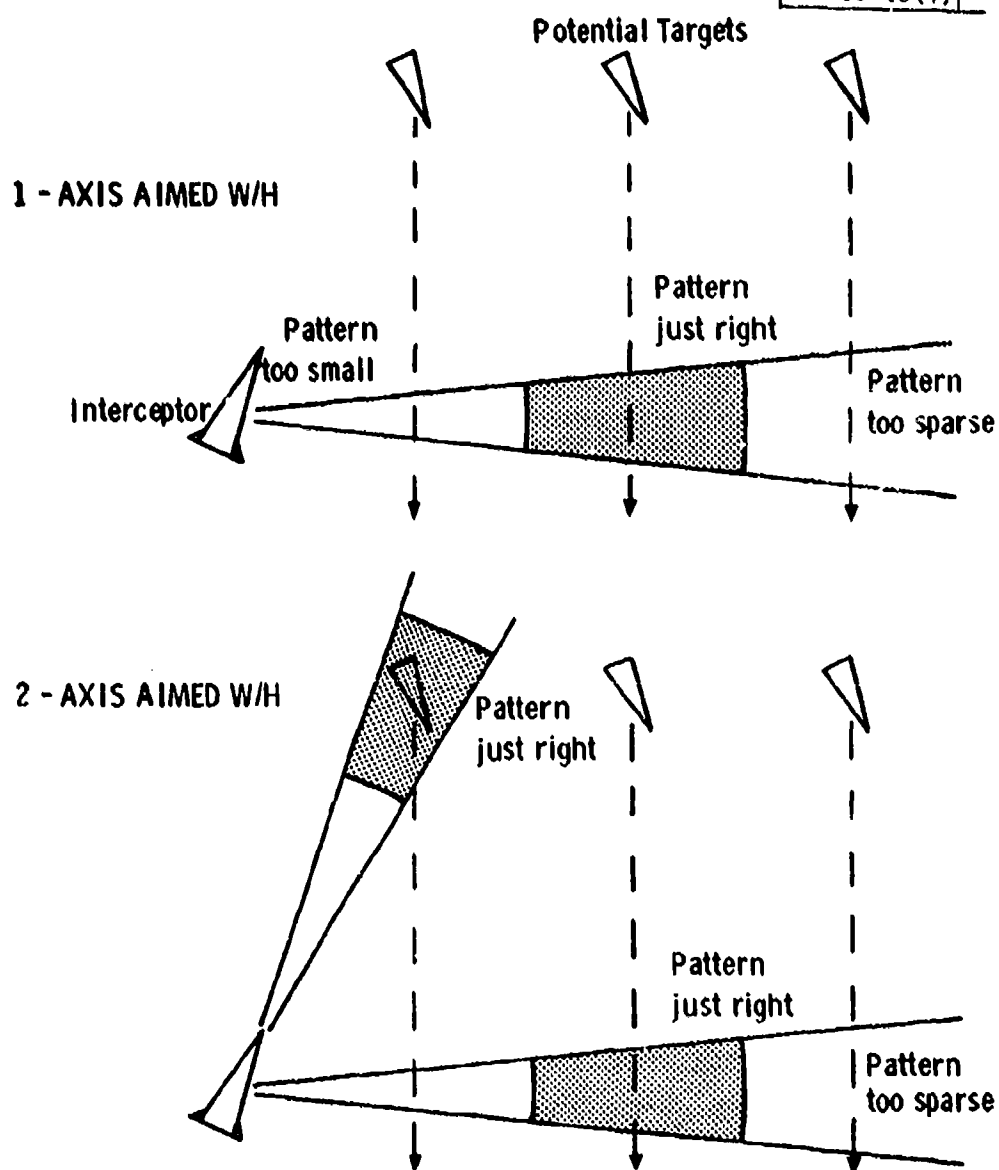just right

Pattern
too sparse

Fig. 7. Intercept geometry in interceptor coordinates.

17

would be the preferred choice. However, two other factors enter
into warhead effectiveness. These are the warhead "coverage"
and response time. We will talk about these below.

The coverage of the warhead is a measure of the un-
certainty volume which can be filled with a sufficient density of
fragments to provide a high kill probability. It is a function
primarily of the number of fragments in the warhead. A narrow
spray angle warhead can operate at large stand-off distances but
its coverage is given by the product of the stand-off distance
and the beamwidth. The resulting pattern size may be smaller
than that of a broader spray-angle warhead or an isotropic warhead.
If the fragment spatial density is fixed by the kill probability
required, the coverage (measured by the unknown error) is propor-
tional to the square root of the number of fragments. Sophisti-
cated warheads generally require complicated aiming mechanisms
which reduce the weight available for fragments. Thus we expect
warheads with greater reach to have smaller coverage. (This is a
generalization and the numerical results for any case depend on the
specific warhead design.)

The third warhead performance measure is the response
time. This is the time prior to kill at which the final decision
must be made regarding warhead aiming and firing. Again we expect
more sophisticated (or flexible) warheads to require more time for
aiming and firing than do simpler warheads.

In the format of Fig. 4, we can characterize a given warhead by its three parameters as shown in Fig. 8. Prior to the minimum fuzing range (corresponding to the product of warhead response time and closing velocity), the warhead has the capability of being aimed to cover a miss-distance within its "reach". At (or before) the minimum fuzing range, it must be aimed and fired toward the current best estimate of the kill point. The allowable error in this estimate is the warhead "coverage".

Figure 9 indicates how the warhead capability might vary for the different warhead types discussed. This figure reflects our prejudice that sophisticated warheads will have the greatest reach but that simpler warheads will have shorter response times and greater coverage.

In specific cases, the effective warhead reach or coverage must be reduced as a result of pointing errors or granularity. Furthermore, the time required for aiming the warhead may be a function of how large an angular change is required. These considerations will affect the specific shape of the warhead capability curves and could be factored into a more complete analysis. However, the curves of Fig. 8 and 9 serve to characterize warheads sufficiently well for evaluating overall engagement performance.

In the next section, we will combine the sensor, interceptor and warhead models to describe and evaluate various aspects of NNK engagements.
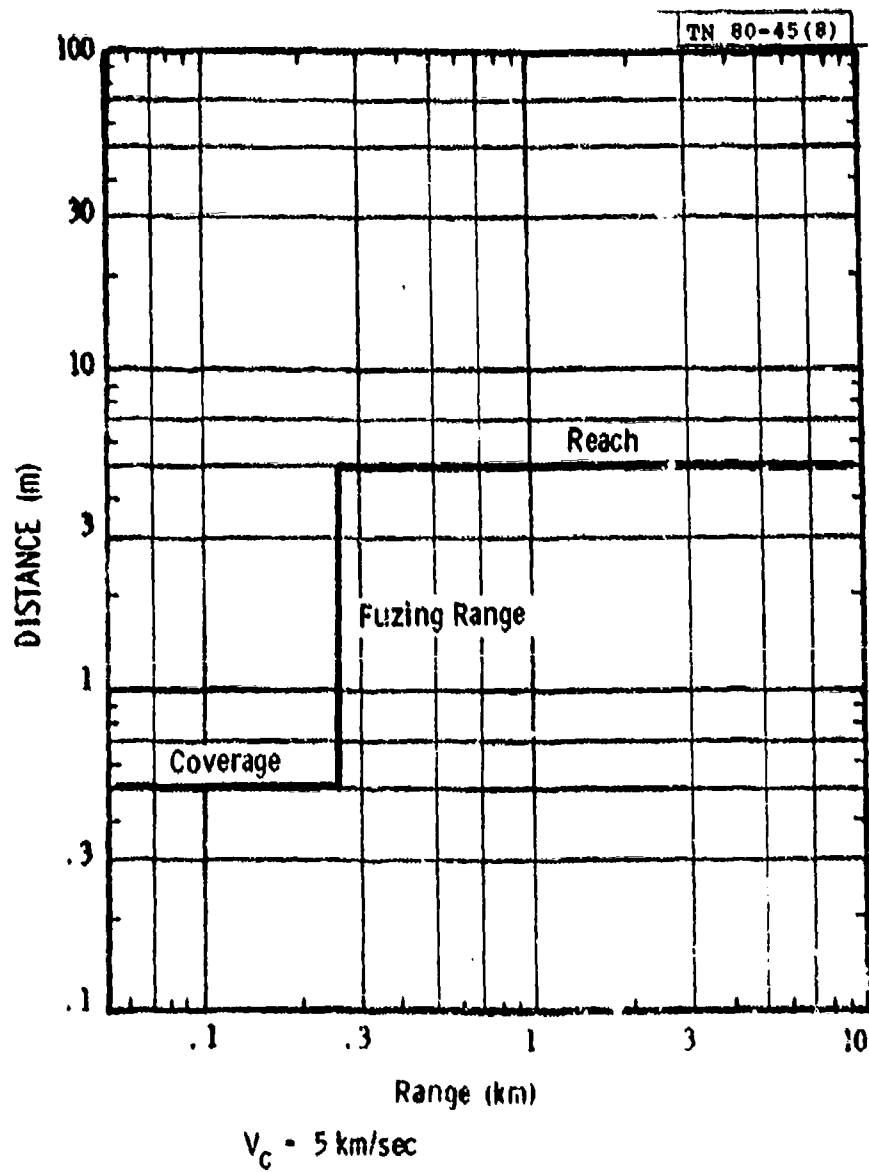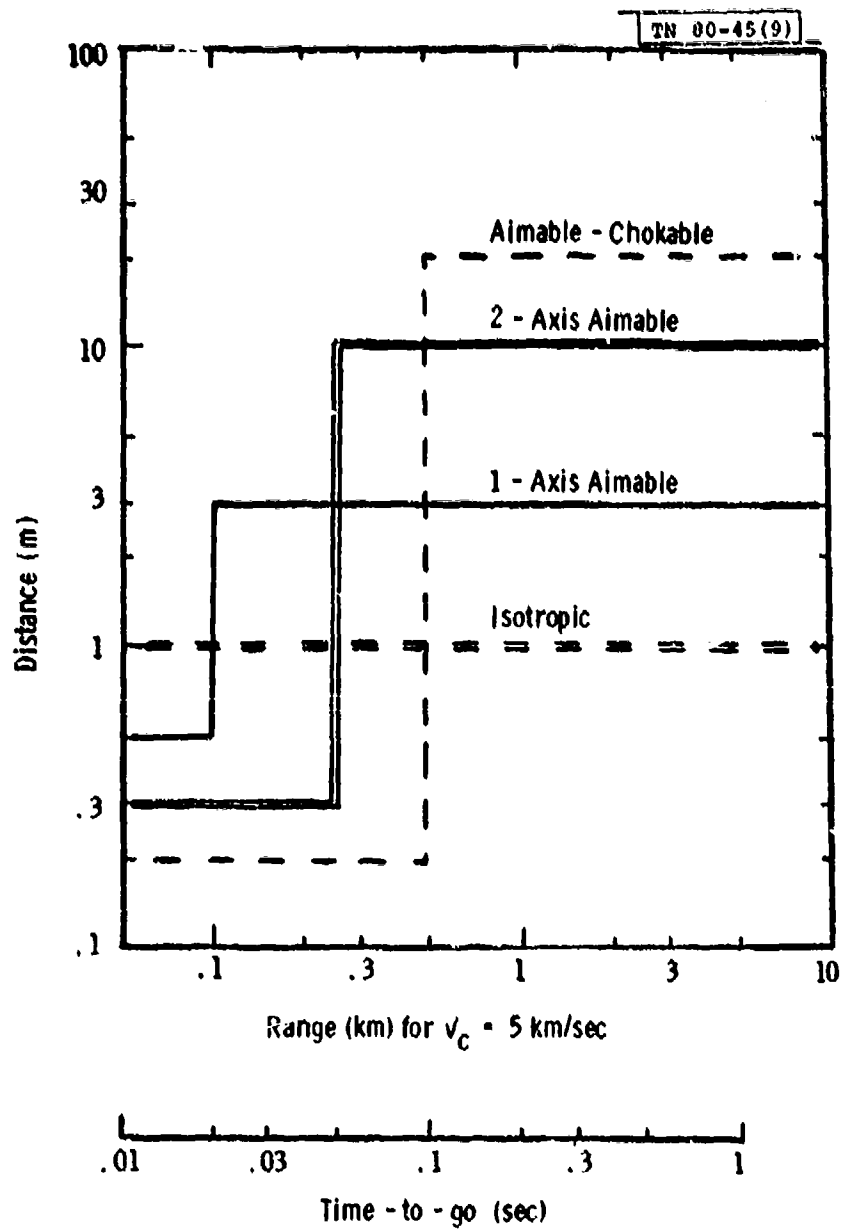
Fig. 8. Warhead characterization.

Fig. 9. Sample warhead parameters.

V. ENGAGEMENT MODEL

Here we extend the model of Ref. [1] to include multiple sensors and various warheads. First we will show a successful engagement to illustrate the model. Following this we will in- dicate various ways in which the engagement can be unsuccessful and how the system must be redesigned to correct these failures. Since there are a large number of parameters characterizing the system components, only sample results will be given. The nomogram kit in Appendix A may be used to analyze a greater variety of cases.

Figure 10 describes a successful engagement; walking through it will indicate how the model is used. An external sensor provides the interceptor with a given handover accuracy prior to seeker acquisition. At point A, the seeker starts making measurements reducing the target prediction error. At point B, the more accurate fuze sensor acquires further reducing the prediction error. Meanwhile, the interceptor divert capability is sufficient to accommodate this sensor prediction error. However, at point C, the interceptor divert capability just equals the prediction error and these quantities provide an estimate of the guidance miss-distance. This guidance miss is within the reach of the warhead (point D) and the system can take advantage of the further decrease in prediction error. Finally at point E, the

decision to fire the warhead must be made. Since the warhead coverage at this time, (point F) is greater than the fuze prediction error, the engagement is successful.

As in Ref. [1], we must emphasize that many of the quantities considered are statistical rather than deterministic and the crossing points of the various curves correspond to expected values or values having a given probability of being exceeded depending on the specific error distribution functions.

From Fig. 10, we can see that there are three primary failure modes for this engagement. If point A lies above the interceptor divert capability curve, we have a handover failure. If point D falls below the prediction error curve, we have a guidance failure. Finally if point F falls below the prediction error curve, we have a fuzing failure. In Fig. 11, we show an example of each type of failure. (All parameters not stated are the same as in Fig. 10.) The remedy for each of these failure modes is to push the interceptor and warhead curves above the prediction error curves. The best way to accomplish this is different for the different failure modes.

To correct a handover failure, the best approaches are to reduce the handover error, increase the interceptor maneuver acceleration or increase the seeker acquisition range. To correct a guidance failure, the best approaches are to decrease the interceptor response time or the seeker angular error or to increase the
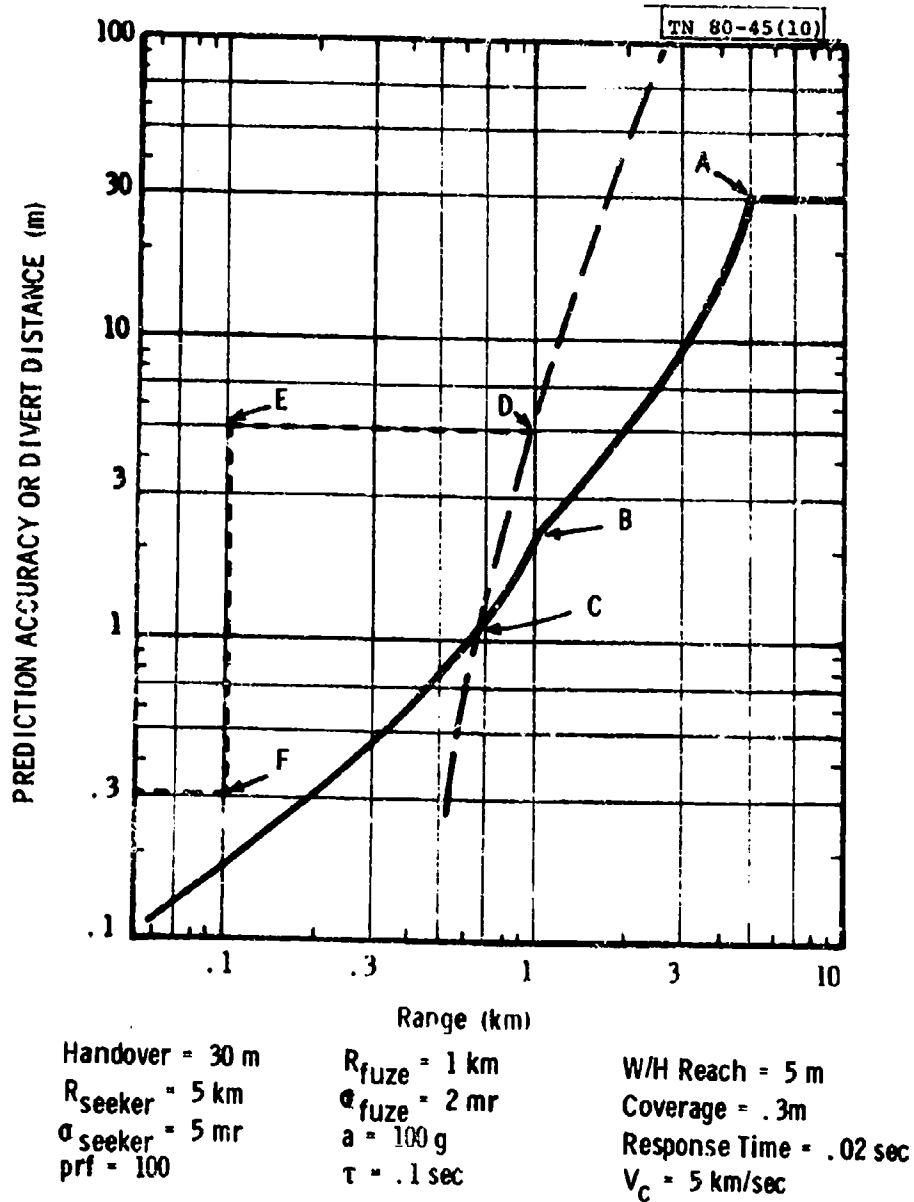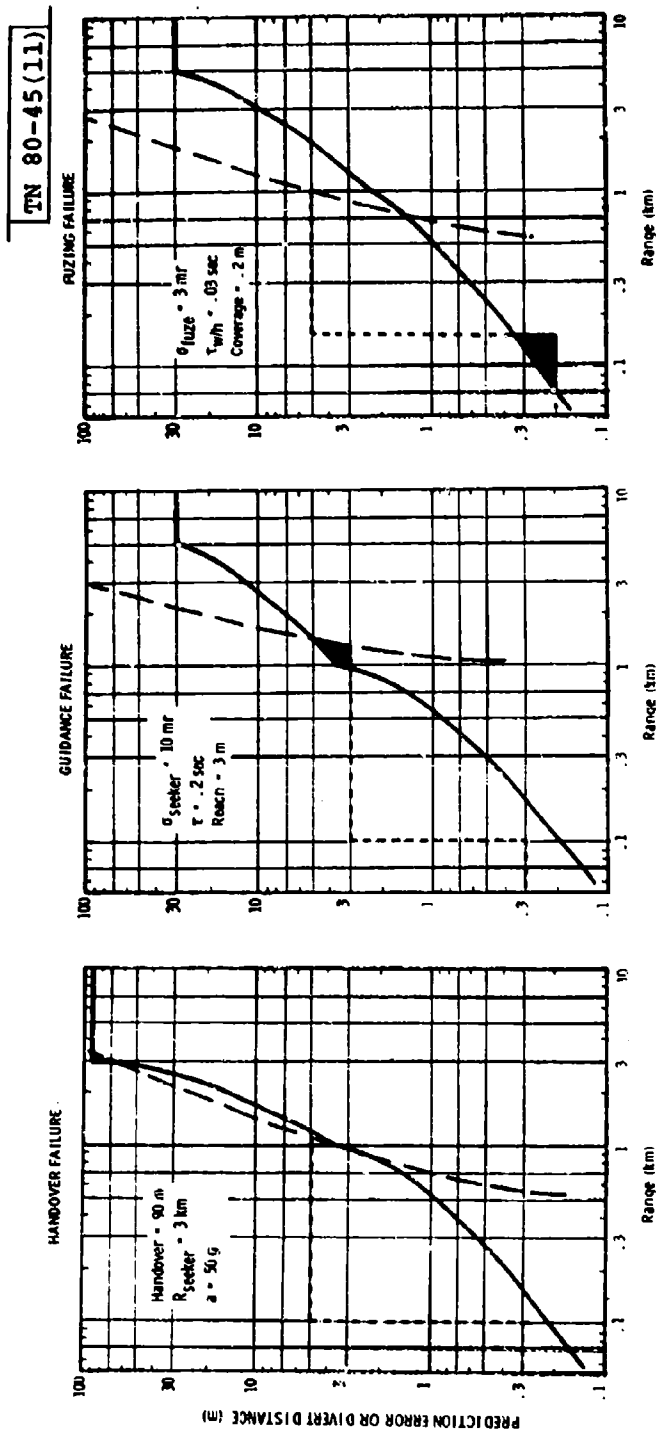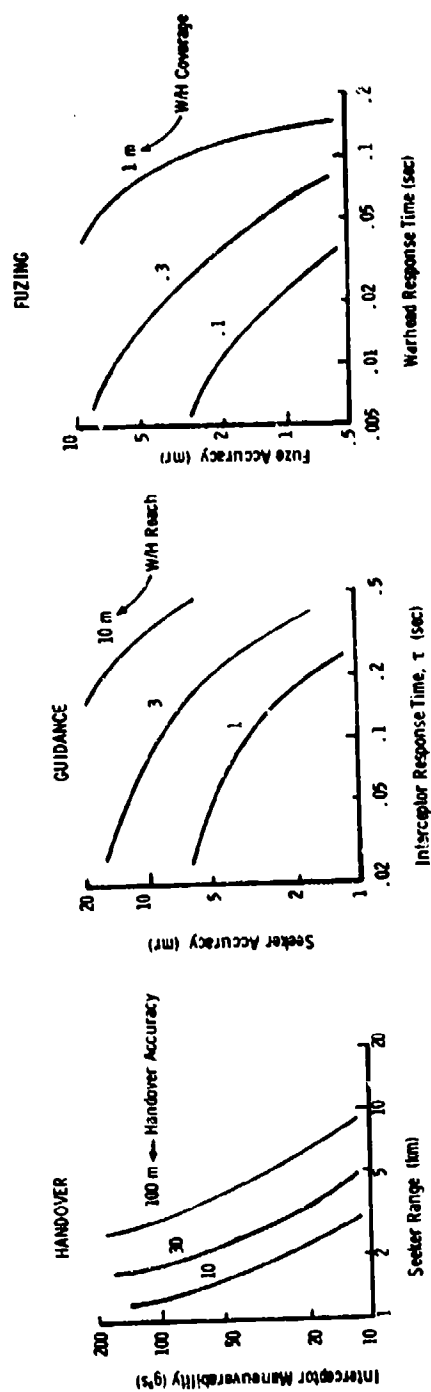
23

Fig. 10. Sample engagement.

Fig. 11. Unsuccessful engagements.

25

warhead reach. To correct a fuzing failure, the best approaches are to reduce the warhead response time or the fuze angular error or to increase the warhead coverage.

Potential parameter trade-offs to solve the problems in Fig. 11 are shown in Fig. 12. These curves were generated using the nomogram in Appendix A. Again these are only meant to be sample results indicating trends rather than definitive system or subsystem requirements.

As a final application of the engagement model, we will consider two cases in which the trade-off of component parameters permits one or more components to be eliminated. If the guidance miss-distance is smaller than the physical dimensions of the inter-ceptor, a direct hit will result and no warhead and fuze will be required; Figure 13a illustrates such a case.

If the handover accuracy is within the reach of the warhead, an onboard seeker is not needed to reduce the guidance miss. A fuzing sensor is needed to fire the warhead but not to guide the interceptor. This case is illustrated in Fig. 13b and would also be appropriate for command guidance where the ground radar prediction accuracy is essentially independent of target-to-interceptor range.
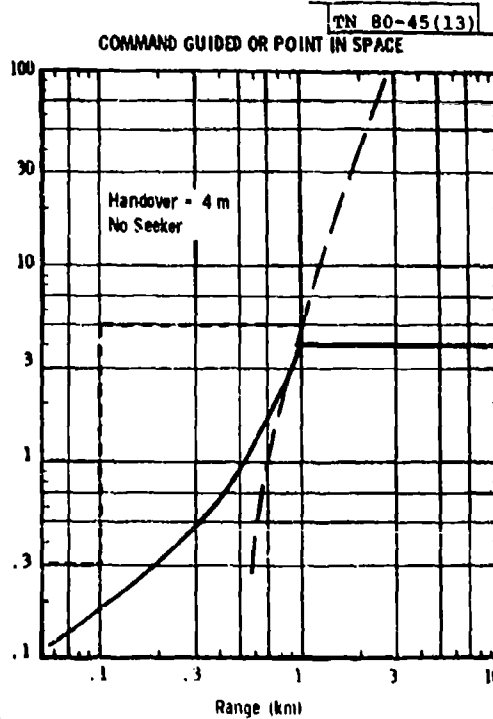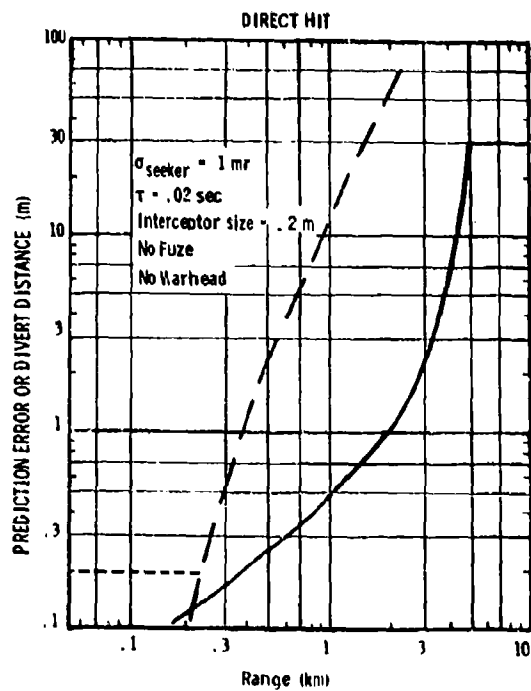
Fig. 12.   Sample trade-offs curves.

TN 80-45 (12)

27

DIRECT HIT

COMMAND GUIDED OR POINT IN SPACE

σ_{seeker} = 1 mr
τ = .02 sec
Interceptor size = .2 m
No Fuze
No Warhead

Handover = 4 m
No Seeker

PREDICTION ERROR OR DIVERT DISTANCE (m)

Range (km)

Range (km)

ALL OTHER PARAMETERS ARE THE SAME AS IN FIG 10

Fig. 13. Other interesting cases.

28

VI. DISCUSSION

In this note, we have presented a simple NNK engagement model including the effects of handover, seeker and fuze acquisition range and accuracy, missile maneuverability and response time and warhead reach, coverage and response time. There are three major stages of an engagement; handover, guidance and fuzing. The handover stage is most strongly influenced by handover accuracy, missile maneuverability and seeker acquisition range. The guidance stage is influenced by the seeker accuracy, the missile response time and the warhead reach. The fuzing stage is influenced by the fuze accuracy and the warhead coverage and response time. All stages of the engagement are affected by the closing velocity.

Using the analysis in the report and particularly the nomograms in Appendix A, it is possible to conduct numerous trade-offs of system and subsystem parameters. While the numerical results obtained are in reasonable agreement with more sophisticated simulation results, they are more useful as an indication of trends and interactions.

APPENDIX A: Nomogram Kit

In this Appendix, we give copies of 6 graphs which may be
made into transparencies and overlayed appropriately to generate
results similar to those given in Ref. [1] and Section V. This
Appendix gives instructions for making and using these nomograms.

Figure A-1 is the base graph with two scales A-A and B-B
giving various values of V_c. Figures A-2 and A-5 contain graphs
of prediction accuracy vs. range for 5 values of acquisition range,
R_A. Figure A-2 corresponds to instrumentation error which was
used in Section V. Figures A-3 through A-5 correspond to other
types of error and were discussed in Ref. [1]. Scale A-A on these
figures should be overlayed on scale A-A on Fig. A-1 with the
appropriate value of $\sigma/\sqrt{prf/100}$ opposite the appropriate value
of V_c. For a prf of 100, the values on scale A-A are just the
measurement accuracies. For higher or lower values of prf, the
effective measurement error will be lower or higher respectively.
Using the appropriate combination of curves, the user can construct
composite prediction error curves similar to those in Section II.

Figure A-6 contains graphs of divert capability vs. range
for 4 values of τ. It also contains 4 horizontal lines for
different maneuver limits and a vertical line for V_c. The
appropriate line for the maneuver limit should be overlayed on
scale B-B on Fig. A-1 and the vertical line should go through
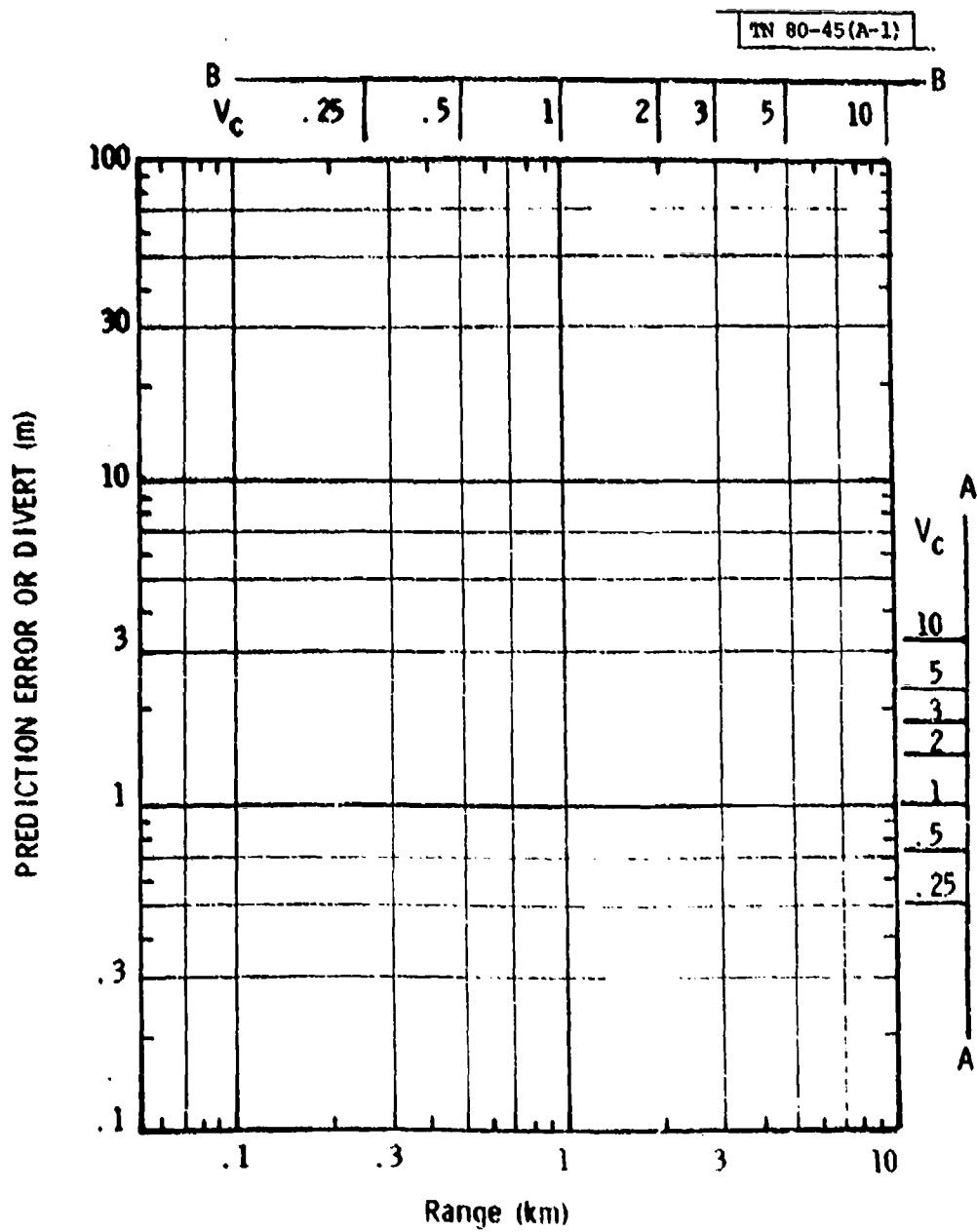the appropriate value of V_c on scale B-B.
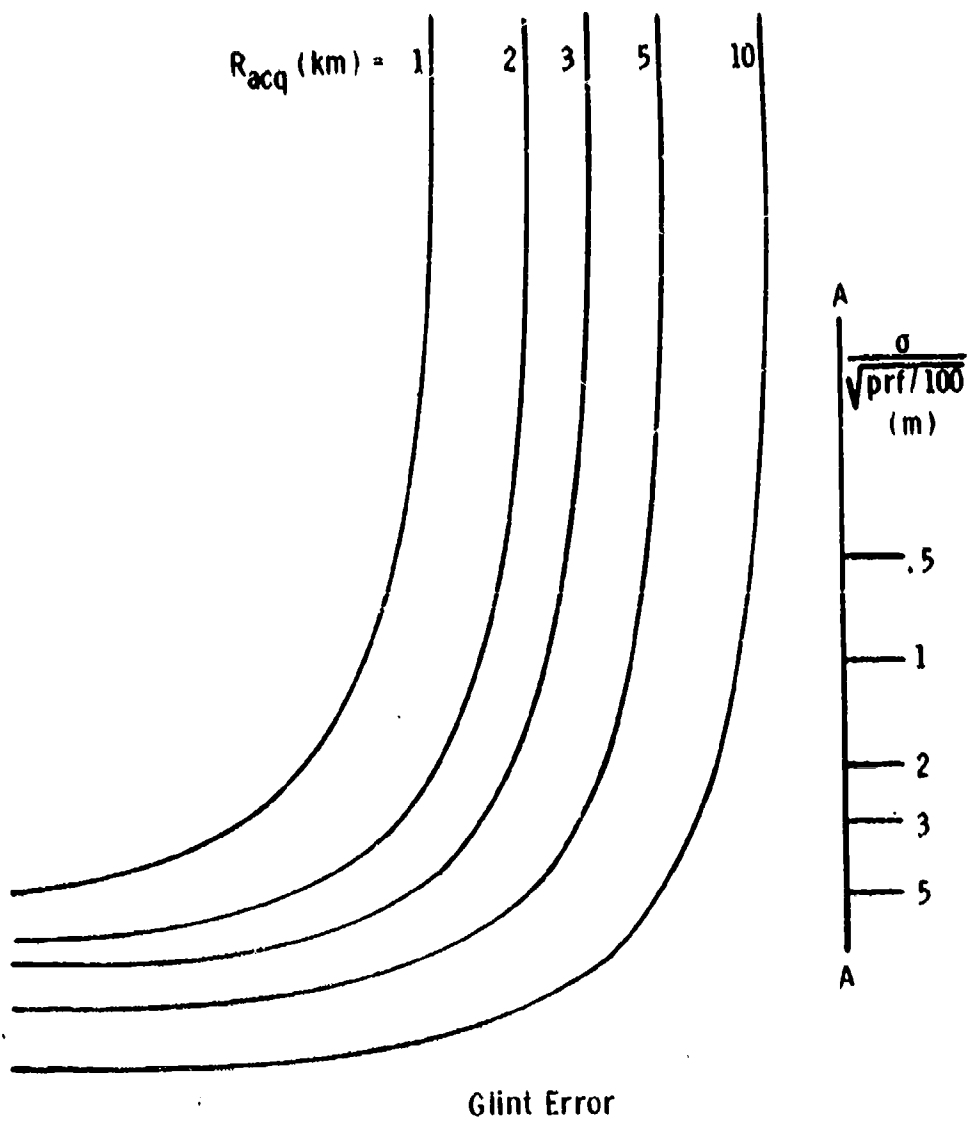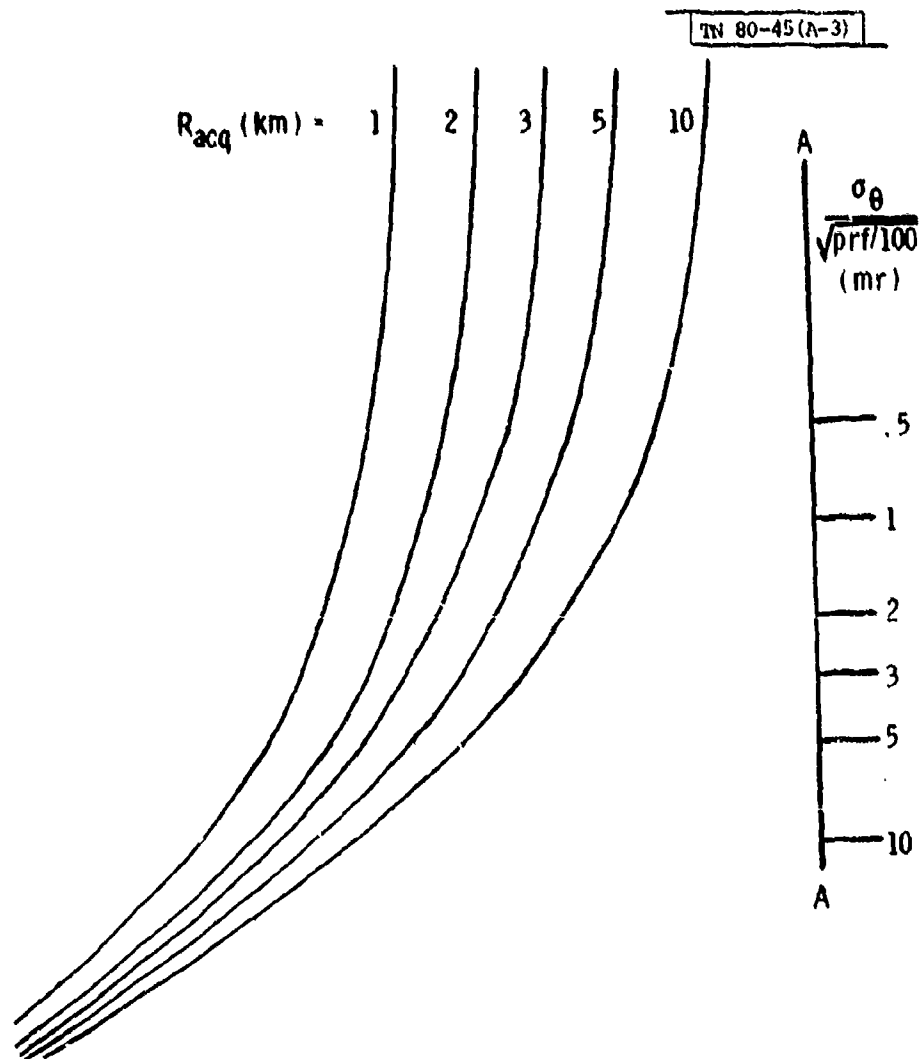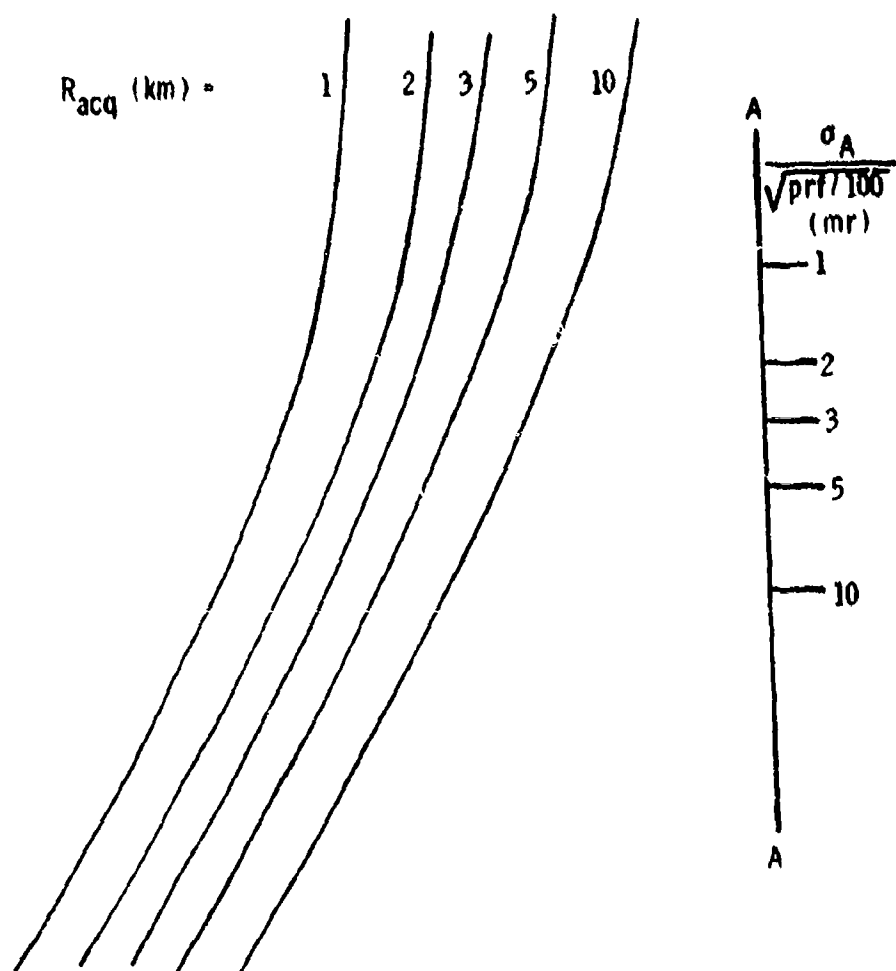
30

Fig. A-1. Nomogram base.

31

R_{acq} (km) = 1   2 3 5   10

A

$$\frac{\sigma}{\sqrt{prf/100}}$$
(m)

.5

1

2

3

5

A

Glint Error

Fig. A-2. Glint overlay.

Instrumentation Error

Fig. A-3. Instrumentation overlay.

R_{acq} (km) =   1   2   3   5   10

A

$$\frac{\sigma_A}{\sqrt{prf/100}}$$
(mr)

1

2

3

5

10

A

Thermal Error (Semi-active)

Fig. A-4.   Thermal (semi-active) overlay.

$$A \quad \frac{\sigma_A}{\sqrt{\text{prf}/100}}$$

(mr)

R_{acq} (km) = 1   2   3   5   10

.5

1

2

3

5

10

A
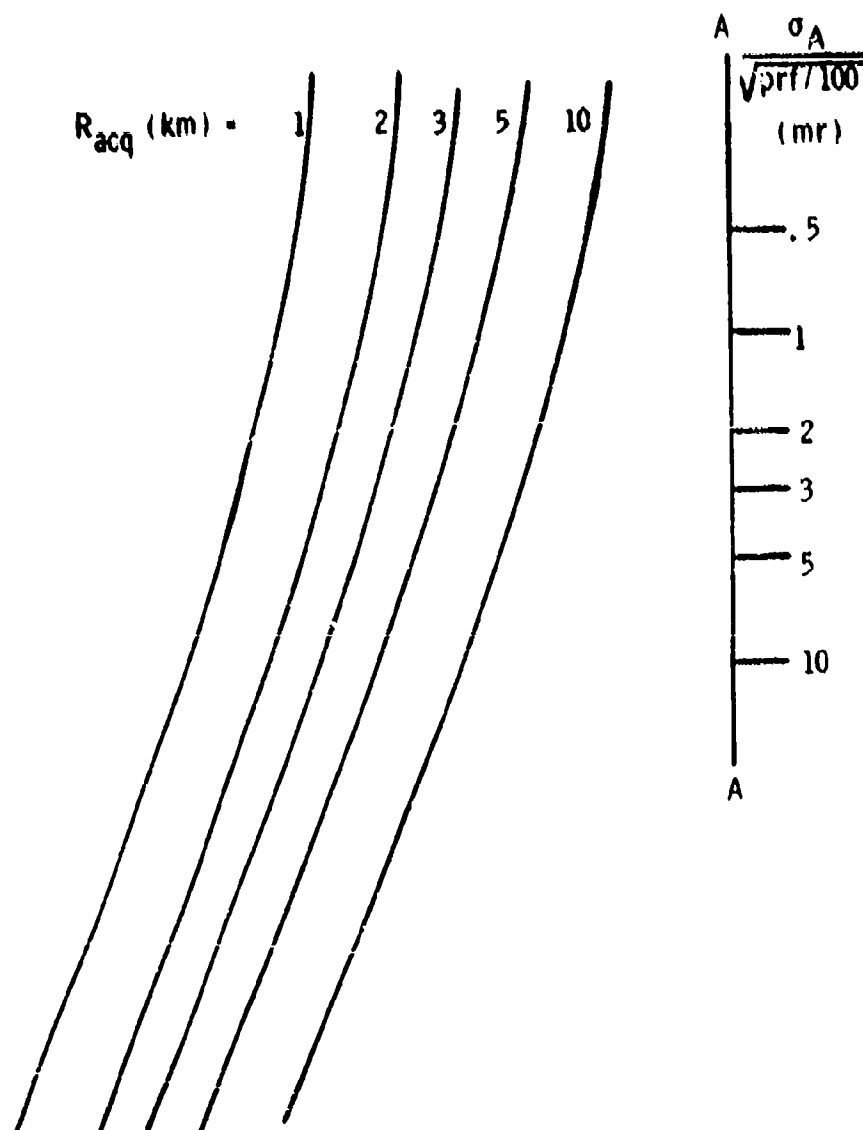
Thermal Error (Active)

Fig. A-5. Thermal (active) overlay.

35
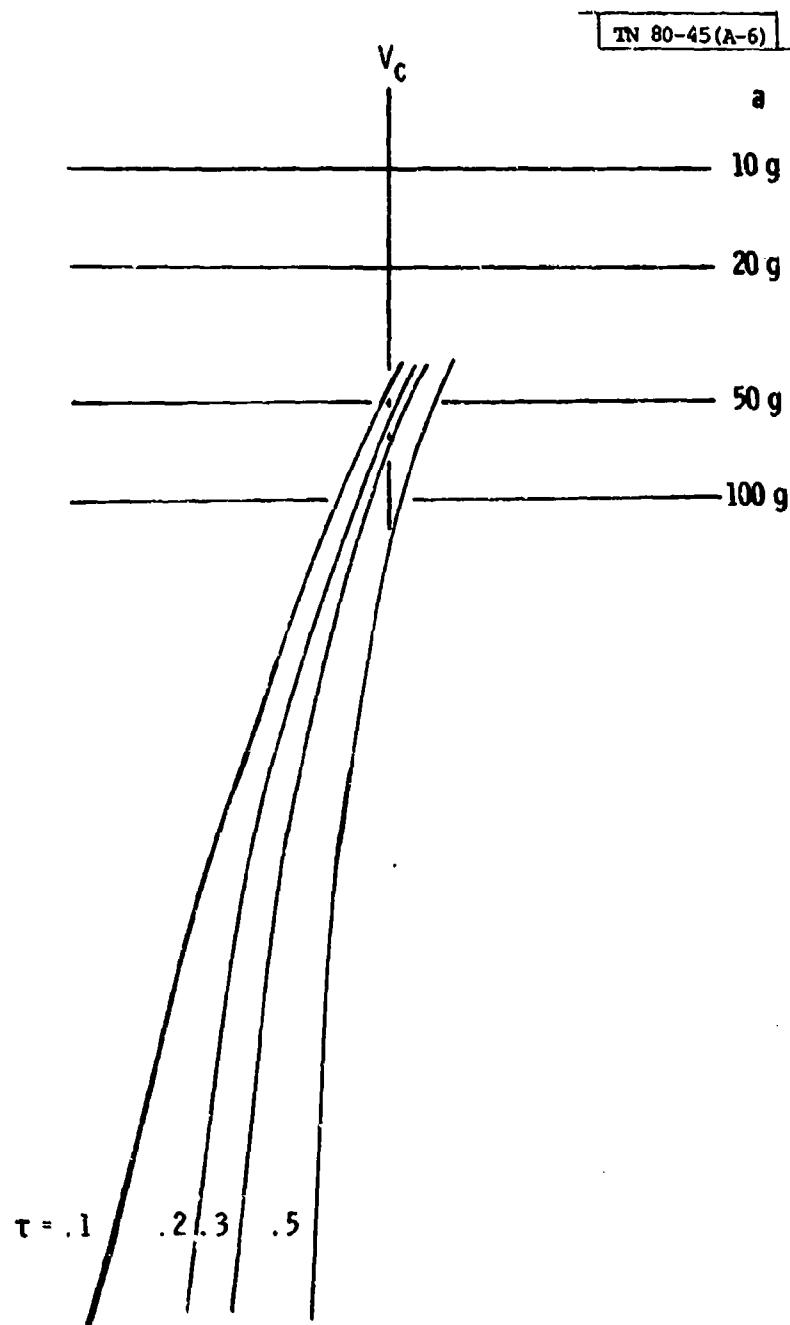
Fig. A-6. Interceptor overlay.

ACKNOWLEDGMENT

37

REFERENCES

1. S. D. Weiner, "A Simple Graphical Model for Analyzing Radar
    Homing Interceptor Engagements", Technical Note, TN-1979-82,
    Lincoln Laboratory, M.I.T., (17 December 1979)   DTIC-AD A082460/7.

2. R. W. Miller and C. B. Chang, "Some Analytical Methods for
    Tracking, Prediction and Interception Performance Evaluations",
    (9 August 1977), (not generally available).

3. C. B. Chang, "Miss Distance and Fuzing Error; Comparison of
    Active and Semi-Active Homing", (7 August 1980), (not generally
    available).

4. R. W. Miller and C. B. Chang, "NNK Interceptor Warhead and
    Fuze Requirements", (14 December 1977), (not generally
    available).

5. C. B. Chang and L. C. Kramer, "Requirements and Success
    Criteria for NNK Engagements", (24 October 1978), (not
    generally available).

SECURITY CLASSIFICATION OF THIS PAGE *(When Data Entered)*

REPORT DOCUMENTATION PAGE	READ INSTRUCTIONS BEFORE COMPLETING FORM

1. REPORT NUMBER	2. GOVT ACCESSION NO.	3. RECIPIENT'S CATALOG NUMBER
ESD-TR-80-186	AD-A093	

4. TITLE *(and Subtitle)*	5. TYPE OF REPORT & PERIOD COVERED
A Model of Interceptor Engagements Including Warhead and Fuze Interactions.	Technical Note
	6. PERFORMING ORG. REPORT NUMBER
	Technical Note 1980-45

7. AUTHOR(s)	8. CONTRACT OR GRANT NUMBER(s)
Stephen D. Weiner	F19628-80-C-0002

9. PERFORMING ORGANIZATION NAME AND ADDRESS	10. PROGRAM ELEMENT, PROJECT, TASK AREA & WORK UNIT NUMBERS
Lincoln Laboratory, M.I.T. P.O. Box 73 Lexington, MA 02173	Program Element Nos. 63304A-63308A

11. CONTROLLING OFFICE NAME AND ADDRESS	12. REPORT DATE
Ballistic Missile Defense Program Office Department of the Army 5001 Eisenhower Avenue Alexandria, VA 22333	18 September 1980
	13. NUMBER OF PAGES
	46

14. MONITORING AGENCY NAME & ADDRESS *(if different from Controlling Office)*	15. SECURITY CLASS. *(of this report)*
Electronic Systems Division Hanscom AFB Bedford, MA 01731	Unclassified
	15a. DECLASSIFICATION DOWNGRADING SCHEDULE

16. DISTRIBUTION STATEMENT *(of this Report)*

Approved for public release; distribution unlimited.

17. DISTRIBUTION STATEMENT *(of the abstract entered in Block 20, if different from Report)*

18. SUPPLEMENTARY NOTES

None

19. KEY WORDS *(Continue on reverse side if necessary and identify by block number)*

non-nuclear interception	interceptor engagements
homing sensors	fuzing sensors
warheads	ballistic missile defense

20. ABSTRACT *(Continue on reverse side if necessary and identify by block number)*

This note represents an extension of previous work on radar homing interceptors to include effects of multiple sensor interactions and the use of aimed warheads to compensate for large guidance miss-distances. Using simple graphical techniques, we treat combinations of data from handover, homing and fuzing sensors. We also consider various types of warheads including isotropic, aimed in one angle, fully aimable and fully aimable and chokable. Sensors are characterized by their accuracy and acquisition range; interceptors by their maneuver capability and response time and warheads by their reach, coverage and response time. We consider some sample intercept engagements and discuss their component requirements.

DD FORM 1473 EDITION OF 1 NOV 65 IS OBSOLETE
1 JAN 73